

Interface Dynamics in Porous Media: A Random-Field Description

J. P. Stokes and A. P. Kushnick

Exxon Research and Engineering Co., Annandale, New Jersey 08801

and

Mark O. Robbins

Department of Physics and Astronomy, Johns Hopkins University, Baltimore, Maryland 21218

(Received 11 January 1988)

We report a variety of measurements on fluid interface motion through model porous media. The dynamics shares many features with other systems pinned by random fields. Over a range of pressures randomness pins the interface. In this range there are many metastable interface configurations and relaxation is extremely slow. The dc response outside the pinned region is markedly nonlinear. Oscillations in the pressure occur at constant velocity which reflect the pore geometry.

PACS numbers: 47.55.Mh

A variety of experimental systems have been identified where disorder plays a crucial role in the determination of both static and dynamic properties. Many have been analyzed within the common framework of the random-field model¹ including charge-density-wave (CDW) conductors,² domain walls in magnetic systems,¹ contact-angle hysteresis,³ segregating fluids in porous media,⁴ and flux vortices in type-II superconductors.⁵ All of these systems share certain characteristics. The ground state is not spatially uniform, but varies in response to the disorder. The characteristic length scale of variations depends on the strength and correlation length of the disorder. There are many nearly degenerate metastable states.

In two systems, CDW conductors and type-II superconductors, a force is readily applied which favors motion between these metastable states. For small forces, the systems remain pinned near one of the metastable minima. Above a threshold force F_T , the system is depinned and evolves continuously. In this dynamic state, the effects of disorder are manifested in the dc response (the force-velocity curve), in the ac response, and in the noise spectrum.

In this paper we report a variety of measurements which reveal both the similarities and differences between the dynamics of driven fluid interface motion in disordered systems and other "random-field" systems. There are many metastable positions of the interface. For each we find a substantial range of applied pressures where the interface velocity v is zero. At pressures outside this pinned region, the pressure-velocity relation is markedly nonlinear. At a constant driving pressure, fluctuations in the velocity are observed which reflect details of the disorder: the pore structure in flow through porous media, and the surface heterogeneity or roughness in contact-line motion. Very slow relaxation of the pressure within the pinned region is observed when the velocity of the interface is forced to zero, reflecting the multiplicity

of metastable static states.

The response to an ac pressure also reveals details of the structure. We have made preliminary studies in both pinned and unpinned regions. However, analysis of these data is more complicated than in other systems because the fluid interface can either expand without changing its contact with the solid or translate along the solid.⁶ In addition, the ac permeability of a single fluid in a porous medium varies substantially with frequency in the range of interest.⁶

Another factor which separates flow through porous media from other random-field systems is the presence of disorder on at least two length scales. The interface may be pinned by microscopic heterogeneity at the surface of the pore space as well as larger-scale variations in the size of pores. Since there is evidence that both the pore volume and surface are fractal in some systems,⁷ there may be an infinite hierarchy of relevant length scales for the disorder.

Two different types of experimental systems were studied to separate the effects of pinning by surface heterogeneity and pore size variation. The first class of systems was uniform-radius tubes where only surface heterogeneity enters. The second class of systems was random packs of monodisperse glass beads in Pyrex tubes. These were sintered lightly to make the bead pack rigid without appreciably changing the pore geometry. Monodispersity of the beads ensured that a single length scale controlled the pore space.

The uniform tubes were untreated quartz. Sintered bead packs were boiled in nitric acid before each run to obtain uniform, reproducible surfaces which were strongly water wetted. The degree of contact-angle hysteresis on the beads was difficult to determine precisely. However, the size of the pinned region in the bead packs was consistent with the variation in pore geometry alone, suggesting that contact hysteresis was less important.

The experimental setup was fabricated from rigid

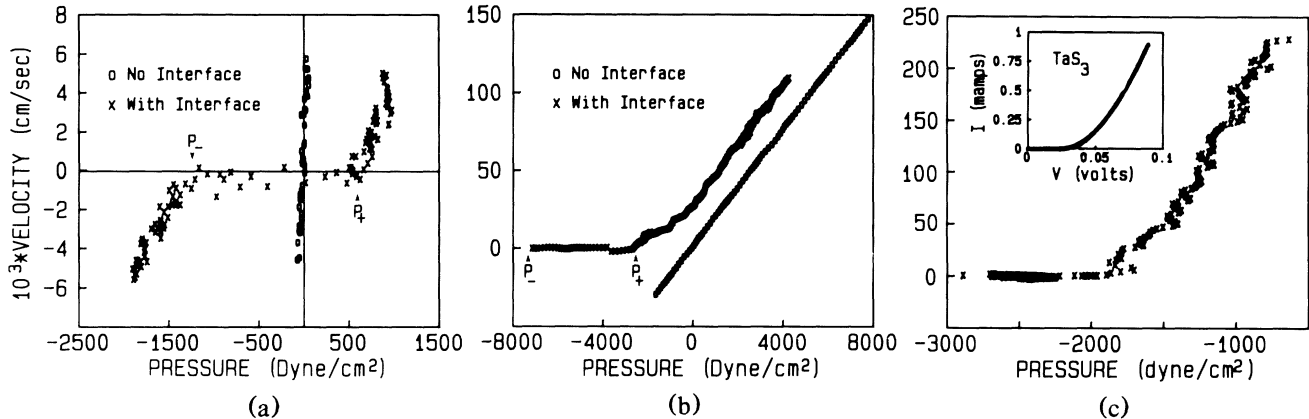


FIG. 1. Velocity vs pressure drop with and without a fluid interface in (a) a 1-mm quartz tube and (b) a 4-mm glass tube packed with 500- μm beads. (c) Bead-pack data with the viscous drop subtracted compared to the CDW current vs voltage for TaS₃ (inset).

glass tubes so that response to changes in pressure was rapid. Fluid velocity in the sample tube was calculated from the pressure drop across a narrow (100–500 μm) tube placed in series. This pressure drop and the drop across the sample tube were measured with use of matched piezoelectric transducers with a sensitivity of at least 100 dyn/cm² (10⁻⁴ atm).

Two fluids with nearly equal viscosities, decane (0.88 cP) and water (0.94 cP), were used. When the wetting fluid (water) displaced the nonwetting fluid (decane), the interface remained fairly flat with fluctuations of order a few bead diameters. Within our accuracy, all of the decane was displaced. In contrast, when the nonwetting fluid displaced the wetting fluid, the interface became very rough and there was substantial fluid trapping.

Figure 1 shows typical dc pressure-velocity plots for (a) a uniform tube and (b) a bead pack. The signs of the pressure and velocity are such that positive values correspond to displacement of decane (nonwetting) by water (wetting). Results for the bead pack were stopped at very small negative velocities, because of the breakup of the interface when the nonwetting fluid displaced the wetting fluid.

With no interface in the samples the dc response is linear and the slope gives the expected absolute mobility $\mu = (\kappa/\eta)A/L$, where κ is the permeability, η is the viscosity, and L and A are the sample length and cross-sectional area. When the interface enters the samples a pronounced pinned region appears. Outside the pinned region the response is highly nonlinear.

The range of pinned pressures in Figs. 1(a) and 1(b) gives information about the type and strength of the disorder. An interface in a tube of radius R is static if the pressure drop across it is $p = 2\gamma\cos\theta/R$ where γ is the surface tension. The contact angle θ is determined by the relative energies of interfaces between the two fluids and between each fluid and the tube.⁸ For a homogene-

ous tube, θ has a unique value. Roughness or chemical heterogeneity leads to a range of values.³ The local contact angle is always consistent with the local surface energy, but the average macroscopic contact angle varies with the position of the contact line.

For the case illustrated in Fig. 1(a), $R = 500 \mu\text{m}$ and $\gamma = 42 \text{ ergs/cm}^2$. Thus the range of pinned pressures corresponds to a range of $\cos\theta$ from -0.41 to 0.71 , or a range of contact angles from about 45° to 115° . The full range of static contact angles was observed visually by the application of an oscillating pressure. There was no apparent motion of the contact line, even though the meniscus moved by more than the tube radius in the tube center.

Interpretation of the pinning pressure in the bead pack is more complicated because it may reflect surface disorder as well as the geometrical disorder of the randomly packed beads. If there is no surface disorder, advance of a nonwetting fluid is pinned at the smallest throats. Detailed solutions for a perfectly nonwetting fluid ($\theta = 180^\circ$) and throats formed by three or four touching beads give critical pressures $p_- \approx -7\gamma/r$, where r is the bead radius.⁹ The dependence of p_- on θ is difficult to calculate. Simple estimates suggest that our measured value $p_- \approx 7 \text{ kdyn/cm}^2 \approx -4\gamma/r$ corresponds to $\theta = 120^\circ$ which is consistent with images of the bead pack.

The pressure at which the velocity becomes positive is determined by different constraints. Advance of a wetting fluid is pinned in the largest throats. The maximum radius one can imagine corresponds to a circle through the centers of beads forming a throat, giving $p_+ \approx p_-/4$. While this agrees with our results, $p_+ \approx 1.7 \text{ kdyn/cm}^2$, the real situation is more complicated. Instability also occurs when the interface hits a new bead which lies ahead of the throat. This and other mechanisms lead to the observed differences in interface shape when the wetting rather than nonwetting fluid advances.¹⁰

To determine the pressure drop due to the interface

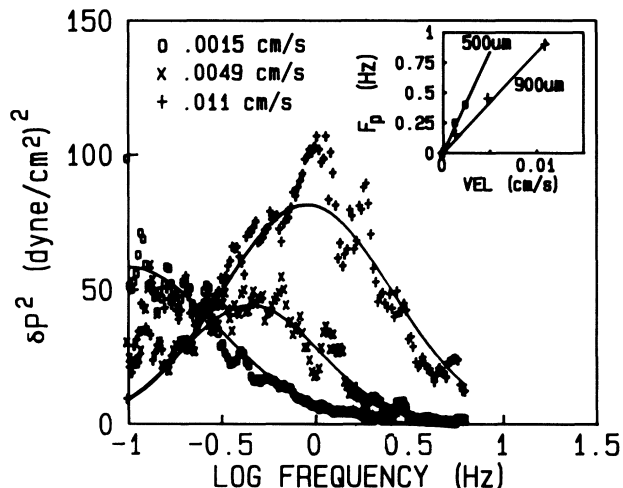


FIG. 2. Power spectrum of the pressure drop in a 900- μm bead pack at the indicated constant velocities and log-normal fits (lines). The slope of the peak frequency vs velocity for 900- and 500- μm beads scales as $1/r$ (inset).

alone, one must subtract the viscous drop across the tube. The result is illustrated in Fig. 1(c) for the bead pack. The pressure drop across the interface increases monotonically and is clearly nonlinear up to the highest velocities shown.

The inset in Fig. 1(c) shows a plot of the CDW current versus voltage in a sample of TaS₃. The qualitative similarity between the two response curves is striking. The details of the nonlinear response are determined both by the forces introduced by the disorder and by the damping mechanism. The latter is different in CDW and fluid systems. Damping in CDW systems is related to scattering by phonons and normal electrons.² Damping in fluids is dominated by the motion of the contact line. This is known to vary with velocity, but because of the singularity associated with the no-slip boundary conditions remains an unsolved theoretical problem.

Disorder affects the response because it produces a fluctuating force on the interface and thus fluctuations in the local velocity. The average damping may be quite different from the damping for motion at the mean velocity if the fluctuations are large and the damping is strongly nonlinear. Since the range of pinned pressures $\Delta p = p_+ - p_-$ is roughly the range of internal forces, velocity fluctuations should be large when the applied pressure exceeds the relevant threshold by less than $\Delta p/2$. Beyond this pressure range the response should mainly reflect damping at the mean velocity.

The internal fluctuations in the force are directly observable as velocity fluctuations at fixed external pressure or pressure fluctuations at fixed flow rate. Figure 2 shows the power spectrum of pressure fluctuations for three constant velocities in a 900- μm bead pack. At

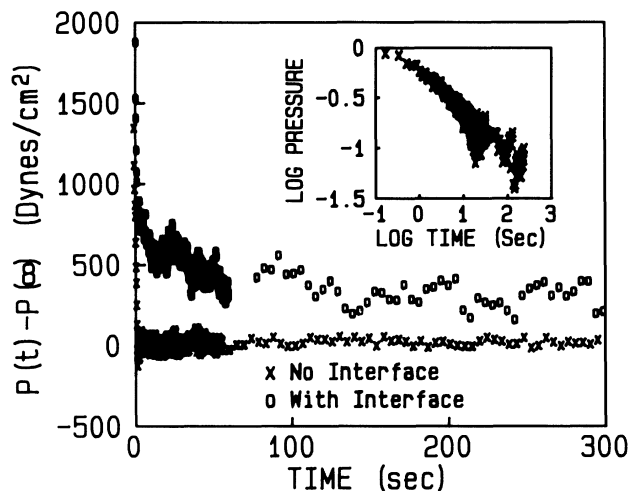


FIG. 3. Decay of the pressure drop after flow is stopped.

each velocity there is an asymmetric peak in the response. The inset shows that the peak frequency scales linearly with velocity and $1/r$.

This noise corresponds to the narrow-band noise in CDW systems, and the peak frequency reflects a characteristic length between pores in the bead pack. The interface moves between pores in a time d_v/v , where v is the average velocity of the interface and d_v is the projection of the pore spacing onto the interface velocity. The power spectrum will show structure at the corresponding frequency v/d_v .

For both $r=250$ - and 500- μm beads the slope of v/w in the inset of Fig. 2 corresponds to $d_v \approx 0.4r$. To understand why this is a characteristic length scale, we consider an fcc structure as a rough model for the bead pack. The fcc structure has tetrahedral and octahedral pores between each plane centered above each of the three possible close-packing sites. The projection of the spacing between centers varies from 0 to $\approx 1.2r$ with the orientation of v . This and the disorder lead to the spread in frequencies in Fig. 2 with a typical frequency near $2v/r$.

Fluctuations in the force on different sections of the interface do not add coherently. The noise is a finite-size effect which should scale as $(\Delta p)^2(\xi^2/A)$ where A is the cross-sectional area of the tube and ξ is a characteristic coherence length for the interface. Preliminary results are consistent with this behavior if ξ is of the order of the bead spacing. No change in the noise power with bead size is observed since $\Delta p \sim 1/r$, $\xi \sim r$, and A is constant.

In a real porous medium there may be many effective pore spacings each producing structure in the noise spectrum. The spectrum will, in general, be broader than in Fig. 2. It may have peaks at several frequencies or exhibit a single broad peak giving the range of length scales. Experiments on more complicated systems are under way.

Interfaces in both bead packs and tubes have many metastable configurations. The interface is visibly rough and different static configurations are observed in the same region of the tube. Roughness is most pronounced in bead packs near p_- , where the nonwetting fluid is trying to advance. The interface can stick at almost any surface formed by contiguous throats. As the pressure increases towards p_+ , the allowed interfaces become flatter.¹⁰

Existence of metastable states can also be observed indirectly in the relaxation of the pressure to its infinite-time limit p_∞ after the velocity is forced to zero by the shutting of a valve. Figure 3 shows the decay of $[p(t) - p_\infty]/[p(0) - p_\infty]$ in a 500- μm bead pack with and without an interface. With no interface complete relaxation occurs in ≈ 2 sec. In contrast, when an interface is in the bead pack the pressure shows an extremely slow decay over more than 300 sec. The inset shows that this decay is fairly linear on a log-log plot, but any fit would depend strongly on the value of p_∞ which is not known accurately. Whatever the precise form, the decay is indicative of a broad distribution of relaxation times suggesting that relaxation occurs through excitation between metastable states.

In most studies of relaxation, the excitation between metastable states is thermally driven.¹¹ In our systems relaxation is not expected to be thermal, since the energy for an interface to move through a pore is $\approx 10^{12}k_B T$. Microscopic motion of the contact line within the pore involves barriers which are orders of magnitude smaller, but still many times $k_B T$. Instead we believe that relaxation is driven by vibrational energy which is coupled to the system. Analysis of the relaxation is difficult until the excitation mechanisms are better understood.

In conclusion, we have shown that the dynamics of fluid interfaces moving over or through disordered solids shares many features with dynamics in other random-field systems: nonlinear dc response, modified ac

response, noise, and metastability. Rough estimates for the scales of these effects have been presented, but further theoretical work is needed to quantify them. Many interesting experimental aspects also remain uninvestigated such as the details of the ac response, and the variation with contact angle and the degree and type of disorder.

We acknowledge useful discussions with S. Bhattacharya, M. Cieplak, P. Dimon, E. Herbolzheimer, and D. A. Weitz. One of us (M.O.R.) also acknowledges support from the National Science Foundation through Grant No. DMR-85-53271 and the Exxon Research Foundation.

¹Y. Imry and S. Ma, Phys. Rev. Lett. **35**, 1399 (1975); G. Grinstein, J. Appl. Phys. **55**, 2371 (1984), and references therein.

²See *Charge Density Waves in Solids*, edited by G. Hutiray and J. Solyom, Lecture Notes in Physics Vol. 217 (Springer-Verlag, Berlin, 1985).

³M. O. Robbins and J. F. Joanny, Europhys. Lett. **3**, 729 (1987).

⁴J. V. Maher, W. I. Goldberg, D. W. Pohl, and M. Lanz, Phys. Rev. Lett. **53**, 60 (1984); D. A. Andelman and J. F. Joanny, in *Physics of Finely Divided Matter*, edited by N. Boccara and M. Daoud (Springer-Verlag, Berlin, 1985), p. 361.

⁵A. T. Fiory, A. F. Hebard, and W. I. Glaberson, Phys. Rev. B **28**, 5075 (1983).

⁶P. Dimon, A. P. Kushnick, and J. P. Stokes, J. Phys. (Paris) (to be published).

⁷A. J. Katz and A. H. Thompson, Phys. Rev. Lett. **54**, 1325 (1985); P.-z. Wong, J. Howard, and J.-S. Lin, Phys. Rev. Lett. **57**, 637 (1986).

⁸P. G. de Gennes, Rev. Mod. Phys. **57**, 827 (1985).

⁹G. Mason and N. R. Morrow, J. Colloid Interface Sci. **100**, 519 (1984).

¹⁰M. Cieplak and M. O. Robbins, to be published.

¹¹P. Dutta and P. M. Horn, Rev. Mod. Phys. **53**, 497 (1981).